

## Japan Concrete Institute TC activities on bond behavior and constitutive laws in RC (Part 2: theoretical behavior by bond laws)

AYasojima & T. Kanakubo  
*University of Tsukuba, Tsukuba, Japan*

H. Shima  
*Kochi University of Technology, Kochi, Japan*

**ABSTRACT:** Bond behavior of reinforced concrete members is influenced by local bond characteristics. This study investigates the theoretical bond behavior and the influence of local bond characteristics on macro-level bond behavior in tensile and pullout specimens by conducting sensitivity analysis based on the second order differential equation derived from force equilibrium and strain compatibility. The bond stress-slip models used are the perfectly rigid-plastic model, the linear model and the parabolic model. Sensitivity analytical results are concluded that the influence of difference between the linear model and the parabolic model is small in the distribution of tensile force and of slip, and maximum tensile load in pullout specimen is influenced by bond length, size and elastic modulus of reinforcing bar and bond fracture energy. It is confirmed that the cross sectional area and the elastic modulus of concrete don't affect the respective distributions.

### 1 INTRODUCTION

Sensitivity analysis by theoretical bond behavior used bond laws is examined as one of the activities of the Japan Concrete Institute Technical Committee on Bond Behavior and Constitutive Laws in Reinforced Concrete. This paper investigates the influence of local bond stress-slip relationship on macro-level bond behavior and bond strength by conducting parametric analysis based on the theoretical solutions derived from the second order differential equation and bond stress-slip models, which is based on force equilibrium and strain compatibility conditions. Local bond stress-slip models, bond length, elastic modulus of reinforcing bar and of concrete, reinforcing bar diameter, concrete cross-sectional area and bond fracture energy are adopted as the factors. In tensile specimen and pullout specimen, the influences of these factors on bond stress distribution, reinforcing bar tensile force distribution, slip distribution and bond strength of pullout specimen are evaluated.

The differential equations governing the bond behavior of a single bar embedded in concrete member (Figure 1) can be summarized as follows, assuming axial symmetry with respect to bar axis. Equation 1 expresses equilibrium in reinforcing bar, and Equation 2 expresses strain-displacement relation, and Equation 3 expresses equilibrium in reinforced concrete. Thus the second order differential equation with respect to the slip is derived from Equation 1, 2 and 3, as represented by Equation 4.

$$\frac{dP_{sx}}{dx} = -\phi_s \cdot \tau_x \quad (1)$$

$$\frac{dS_x}{dx} = -\frac{P_{sx}}{E_s A_s} + \frac{P_{cx}}{E_c A_c} \quad (2)$$

$$P_{sx} + P_{cx} = P_{s0} + P_{c0} \quad (3)$$

$$\frac{d^2 S_x}{dx^2} = \frac{1+np}{E_s A_s} \phi_s \cdot \tau_x \quad (4)$$

Where  $P_{sx}$ = the reinforcing bar force at  $x$ ,  $P_{cx}$ = the concrete force at  $x$ ,  $P_{s0}$ = the reinforcing bar force at  $x = 0$ ,  $P_{c0}$ = the concrete force at  $x = 0$ ,  $E_s$ =the elastic modulus of the reinforcing bar,  $A_s$ = the reinforcing bar area,  $E_c$ = the elastic modulus of the concrete,  $A_c$ = the concrete cross-sectional area,  $n$ = the ratio of the elastic modulus ( $= E_s/E_c$ ),  $p$ = the ratio of area( $=A_s/A_c$ ), and  $\phi_s$ = the reinforcing bar perimeter.

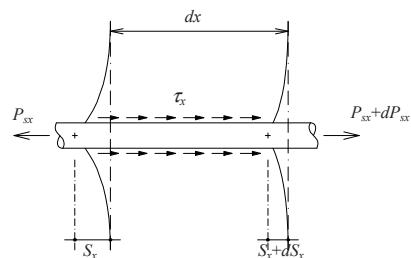


Figure 1. Bond behavior on a minute length of reinforcing bar.

## 2 ANALYSIS METHOD

### 2.1 Bond stress-slip model

To conduct sensitivity analysis by theoretical solution and numerical calculation based on the second order differential equation with respect to the slip, the three bond stress-slip models are used as, illustrated in Figure 2. They are (A) the perfect rigid-plastic model, (B) the linear model, and (C) the parabolic model, defined by the local bond strength ( $\tau_m$ ), the bond stiffness ( $k$ ), and the ultimate slip ( $S_u$ ).

### 2.2 Analyzed specimens

Specimens for sensitivity analysis are the two types. One is a tensile bond specimen with long bond length, and the other is a pullout bond specimen with

bond length ( $l_b$ ). The tensile bond specimen is anchored at the position of  $x = L$  from the end of member, and the slip at that position is set as  $\Delta S = 0.001\text{mm}$  which is close to zero. The outline of analyzed specimens and the boundary conditions on the reinforcing bar force, the concrete force and the slip are shown in Table 1.

### 2.3 Theoretical solution

The theoretical solutions of Equation 4 using the three bond stress-slip model (the perfect rigid-plastic model, the linear model, and the parabolic model) are shown Table 2, 3, 4, 5, and 6. In the pullout bond specimen, the parabolic model cannot solve Equation 4 mathematically. Therefore, the theoretical solution for pullout specimen by the parabolic model is not shown.

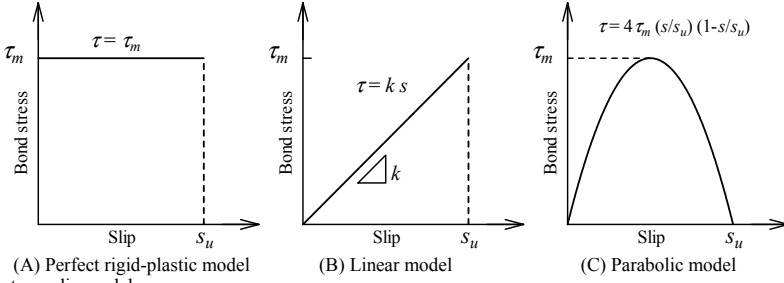


Figure 2. Bond stress-slip models.

Table 1. Analyzed specimens and boundary conditions.

	Target specimens	Boundary conditions
Tensile specimen		$P_{so} = P'_{so}$ and $P_{co} = P'_{co} = 0$ $x = L: S_x(L) = \Delta S$ $x = 0: P_s(0) = P_{so}$ (given value)* $x = L: P_s(L) = P_{so} \cdot np / (1 + np)$
Pullout specimen		$P_{so} = -P_{co}$ and $P'_{so} = P'_{co} = 0$ $x = l_b: S_x(l_b) = S_f$ (given value)* $x = l_b: P_s(l_b) = 0$ $x = l_b: P_c(l_b) = 0$

\* The tensile force of the loaded end ( $P_{so}$ ) and the slip of the free end ( $S_f$ ) are arbitrary (input values).

Table 2. Theoretical solution for perfect rigid-plastic model in tensile specimen.

Bond stress	$\tau_x = \tau_m$
Reinforcing bar force	$P_{sx} = \phi_s \tau_m (L - x) + \frac{np}{1 + np} P_{so}$
Slip	$S_x = \frac{(1 + np) \phi_s \tau_m}{2E_s A_s} (L - x)^2 + \Delta S$
Reinforcing bar force and slip relationship	$P_{sx} = \frac{np}{1 + np} P_{so} + \sqrt{\frac{2E_s A_s \phi_s \tau_m}{1 + np}} (S_x - \Delta S)$
Anchorage length	$L = \frac{P_{so}}{(1 + np) \phi_s \tau_m}$

Table 3. Theoretical solution for perfect rigid-plastic model in pullout specimen.

Axial location	$0 \leq x \leq l_u$	$l_u \leq x \leq l_b$
Bond stress	$\tau_x = 0$	$\tau_x = \tau_m$
Reinforcing bar force	$P_{sx} = \phi_s \tau_m (l_b - l_u)$	$P_{sx} = \phi_s \tau_m (l_b - x)$
Slip	$S_x = \frac{(1+np)\phi_s \tau_m}{E_s A_s} (l_b - l_u)(l_u - x) + S_u$	$S_x = \frac{(1+np)\phi_s \tau_m}{2E_s A_s} (l_b - x)^2 + S_f$
Reinforcing bar force and slip relationship	$P_{sx} = \sqrt{\frac{2E_s A_s \phi_s \tau_m}{1+np} (S_u - S_f)}$	$P_{sx} = \sqrt{\frac{2E_s A_s \phi_s \tau_m}{1+np} (S_x - S_f)}$
Length where bond stress is zero	$l_u = l_b - \sqrt{\frac{2E_s A_s}{(1+np)\phi_s \tau_m} (S_u - S_f)}$	

Table 4. Theoretical solution for linear model in tensile specimen.

Bond stress	$\tau_x = k \frac{\Delta S}{2} (e^{-\alpha(L-x)} + e^{\alpha(L-x)})$
Reinforcing bar force	$P_{sx} = \frac{\alpha E_s A_s}{1+np} \cdot \frac{\Delta S}{2} (-e^{-\alpha(L-x)} + e^{\alpha(L-x)}) + \frac{np}{1+np} P_{so}$
Slip	$S_x = \frac{\Delta S}{2} (e^{-\alpha(L-x)} + e^{\alpha(L-x)})$
Reinforcing bar force and slip relationship	$P_{sx} = \frac{\alpha E_s A_s}{1+np} \sqrt{(S_x^2 - \Delta S^2)} + \frac{np}{1+np} P_{so}$
Anchorage length and Notation of the equations	$L = \frac{1}{\alpha} \ln \left( P_{so} / (\alpha E_s A_s \Delta S) + \sqrt{(P_{so} / (\alpha E_s A_s \Delta S))^2 + 1} \right) \alpha = \sqrt{\frac{k(1+np)\phi_s}{E_s A_s}}$

Table 5. Theoretical solution for linear model in pullout specimen.

Axial location	$0 \leq x \leq l_u$	$l_u \leq x \leq l_b$
Bond stress	$\tau_x = 0$	$\tau_x = k \frac{S_f}{2} (e^{-\alpha(l_b-x)} + e^{\alpha(l_b-x)})$
Reinforcing bar force	$P_{sx} = \frac{\alpha E_s A_s}{1+np} \cdot \frac{S_f}{2} (-e^{-\alpha(l_b-l_u)} + e^{\alpha(l_b-l_u)})$	$P_{sx} = \frac{\alpha E_s A_s}{1+np} \cdot \frac{S_f}{2} (-e^{-\alpha(l_b-x)} + e^{\alpha(l_b-x)})$
Slip	$S_x = \frac{\alpha S_f}{2} (-e^{-\alpha(l_b-l_u)} + e^{\alpha(l_b-l_u)})(l_u - x) + S_u$	$S_x = \frac{S_f}{2} (e^{-\alpha(l_b-x)} + e^{\alpha(l_b-x)})$
Reinforcing bar force and slip relationship	$P_{sx} = \frac{\alpha E_s A_s}{1+np} \sqrt{(S_x^2 - S_f^2)}$	$P_{sx} = \frac{\alpha E_s A_s}{1+np} \sqrt{(S_x^2 - S_f^2)}$
Length where bond stress is zero and Notation	$l_u = l_b - \frac{1}{\alpha} \ln \left( S_u / S_f + \sqrt{(S_u / S_f)^2 - 1} \right) \alpha = \sqrt{\frac{k(1+np)\phi_s}{E_s A_s}}$	

Table 6. Theoretical solution for parabolic model in tensile specimen.

Bond stress	$\tau_x = 24\tau_m \frac{X(X^2 - 4X + 1)}{(X+1)^4}$
Reinforcing bar force	$P_{sx} = \frac{E_s A_s}{1+np} \left( \frac{6\beta \cdot X(X-1) \cdot S_u}{(X+1)^3} \right) + \frac{np}{1+np} P_{so}$
Slip	$S_x = \frac{6X}{(X+1)^2} S_u$
Reinforcing bar force and slip relationship	$P_{sx} = \sqrt{\frac{4E_s A_s \phi_s \tau_m S_u}{1+np} \cdot \left( \frac{S_x}{S_u} \sqrt{1 - \frac{2S_x}{3S_u}} \right)} + \frac{np}{1+np} P_{so}$
Anchorage length, Condition of loaded-end force and Notations	$L = \frac{1}{\beta} \ln \left[ 3S_u / (2\Delta S) \left( 1 + \sqrt{1 - 2\Delta S / (3S_u)} \right)^2 \right] - C_1$ $P_{so} \leq \sqrt{\frac{4}{3}} (1+np) E_s A_s \phi_s \tau_m S_u$ $X = e^{\beta(x+C_1)}$ $\beta = \sqrt{4(1+np)\phi_s \tau_m / (E_s A_s S_u)}$ $C_1 = \frac{1}{\beta} \ln \left[ (Z_1 + iZ_2)^{1/3} + (Z_1 - iZ_2)^{1/3} + D - 1 \right]$ $Z_1 = D \cdot (2D^2 - 9D + 6) / 2$ $Z_2 = \frac{D}{2} \sqrt{3(D^2 - 12)}$ $D = 2E_s A_s \cdot \beta \cdot S_u / P_{so}$

The solution method used for the parabolic model in the pullout specimen is the sequential integration method in which numerical calculations are performed base on force equilibrium and deformation compatibility conditions, assuming that local bond stress of the infinitesimal length is constant.

### 3 RESULTS OF SENSITIVITY ANALYSIS

#### 3.1 Bond behavior in tensile specimen

The bond behavior results obtained by the each models are shown in Figure 3 and Figure 4, which illustrates the models and factors, bond stress distribution, reinforcing bar tensile force distribution, and slip distribution with distance from the loaded end of tensile specimen. The specifications of analysis factors are set as the cross section of specimen  $100\text{mm} \times 100\text{mm}$  or  $300\text{mm} \times 300\text{mm}$  which contains deformed bar D10 or D19 in the center (elastic modulus,  $E_s = 200\text{GPa}$ ), the elastic modulus of the concrete  $E_c = 20\text{GPa}$  or  $40\text{GPa}$ , local bond strength  $10\text{MPa}$  or  $20\text{MPa}$ , bond stiffness  $20\text{MPa/mm}$  or  $40\text{MPa/mm}$ , ultimate slip of the parabolic model  $0.5\text{mm}$  or  $1.0\text{mm}$ .

From the bond behavior obtained by the each model, the linear model and the parabolic model

give similar distributions of bond stress and of tensile force, however, the bond stress of parabolic model at  $P_{so} = 46\text{ kN}$  decreases near the loaded end in the left side distributions of Figure 3, and all models give similar shape of slip distribution except the value of slip at the loaded-end. In the perfect rigid-plastic model, it is confirmed that bond stress distribution is constant, tensile force distribution is linear, slip distribution is parabolic, and each distribution is confined to the limited length of the reinforcing bar.

When the local bond strength and the bond stiffness vary, the region where the bond stress occurs significantly varies in all the models and the bond stress and the slip near loaded end change; however, the shapes of tensile force distribution and of slip distribution vary little among the linear model and the parabolic model.

It is confirmed that the cross sectional area of the specimen and the elastic modulus of concrete don't affect the respective distributions.

In case of the specimen cross section  $300\text{mm} \times 300\text{mm}$  which contains deformed bar D19 in the center, the perfect rigid-plastic model and the parabolic model give relatively similar distributions of bond stress and of tensile force, and the shape of slip distribution is similar for all the models except the loaded-end slip.

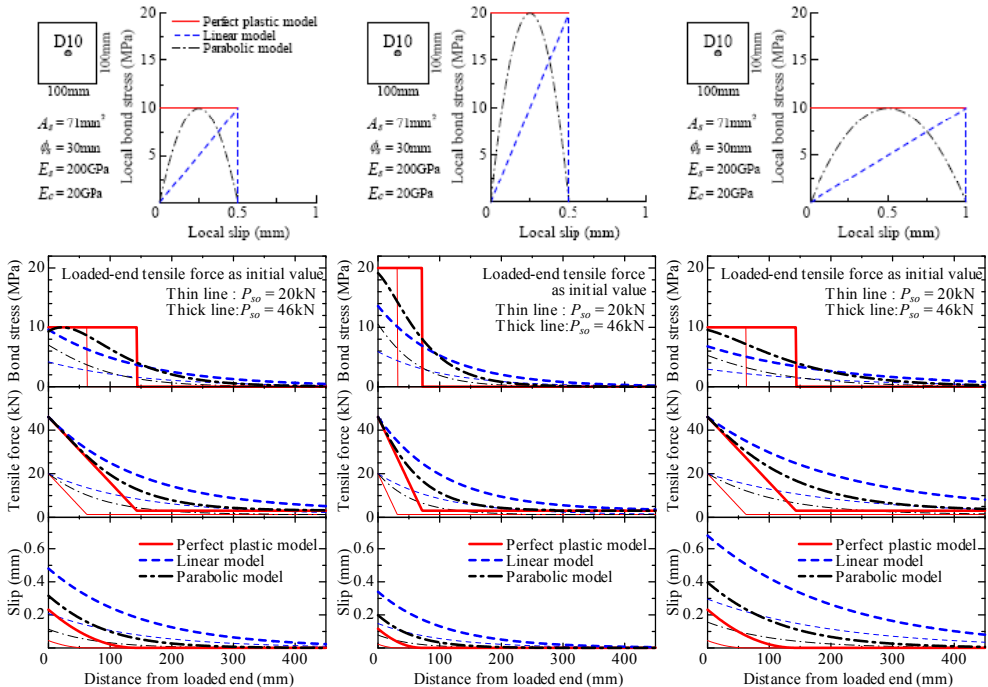


Figure 3. Bond stress-slip model, Bond stress distribution, Tensile force distribution and Slip distribution in tensile specimen.

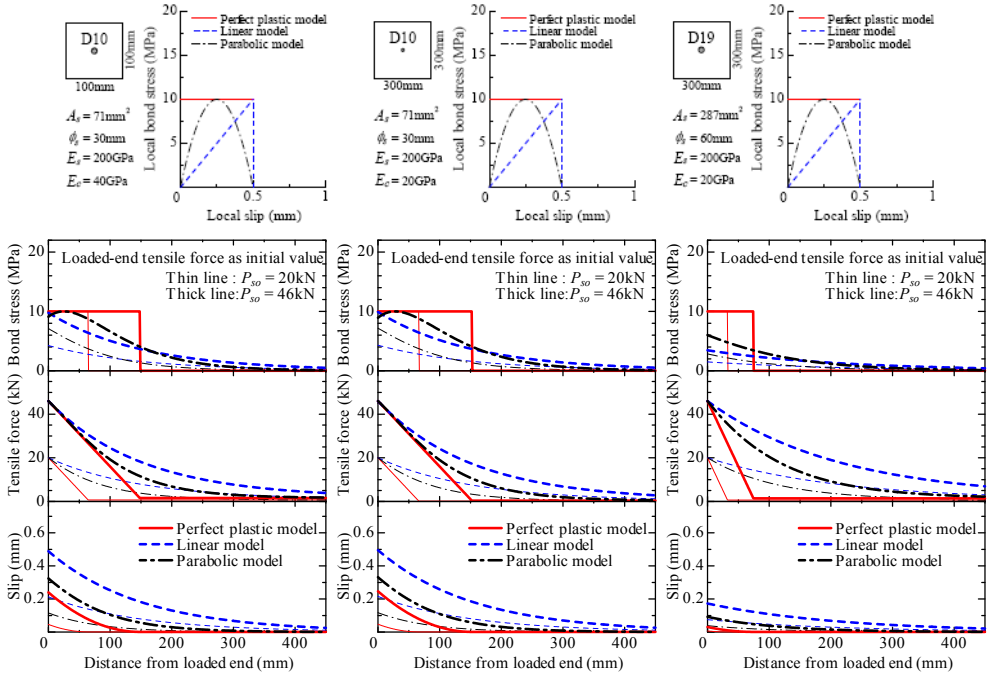


Figure 4. Bond stress-slip model, Bond stress distribution, Tensile force distribution and Slip distribution in tensile specimen.

### 3.2 Bond behavior in pullout specimen

The analysis results of bond behavior obtained by the each models are shown in Figure 5, which illustrates the models and factors, the relationship between loaded-end tensile load and loaded-end slip, bond stress distribution, reinforcing bar tensile force distribution, and slip distribution with distance from the loaded end of pullout specimen. The bond behavior results for the parabolic model are obtained by numerical calculations.

The specifications of analysis factors are set as the cross section of specimen 100 mm × 100 mm or 300 mm × 300 mm which contains deformed bar D10 or D19 in the center (elastic modulus,  $E_s = 200\text{GPa}$ ), the elastic modulus of the concrete  $E_c = 20\text{GPa}$  or  $40\text{GPa}$ , bond length  $l_b = 200\text{mm}$  or  $400\text{mm}$ , local bond strength 10MPa or 20MPa, bond stiffness 20MPa/mm or 40MPa/mm, and ultimate slip 0.5mm.

In comparison with relationship between the tensile load and the loaded-end slip calculated by the each model, the tensile load appears to be related to the shape of the local bond stress-slip relationship, as the perfect rigid-plastic model has the highest maximum tensile load, followed by the parabolic model and, finally, the linear model.

From the bond behavior results obtained by the each model, the bond stress distribution differs among the models, and the length where the bond stress occurs is influenced by the local bond stress-slip model. However, the slip distribution is similar for all models, and the tensile force distribution comes to be alike as the free-end slip becomes larger.

When the local bond strength for the each model doubles from 10MPa to 20MPa, the maximum tensile load increases about 1.5 times in all the models and the slip near the loaded-end increases significantly, and it is confirmed that the cross sectional area of the specimen and the elastic modulus of concrete don't affect the respective distributions.

In case of the specimen cross section 300 mm × 300 mm which contains deformed bar D19 in the center, the perfect rigid-plastic model and the parabolic model give similar distributions of bond stress and of tensile force, and the slip distribution is quite similar for all the models. It is confirmed that the increase of bond length from 200mm to 400mm causes the location of the peak bond stress to shift toward the free end of the reinforcing bar, the distribution of tensile force near the loaded end to remain constant, and the slip near the loaded end to increase.

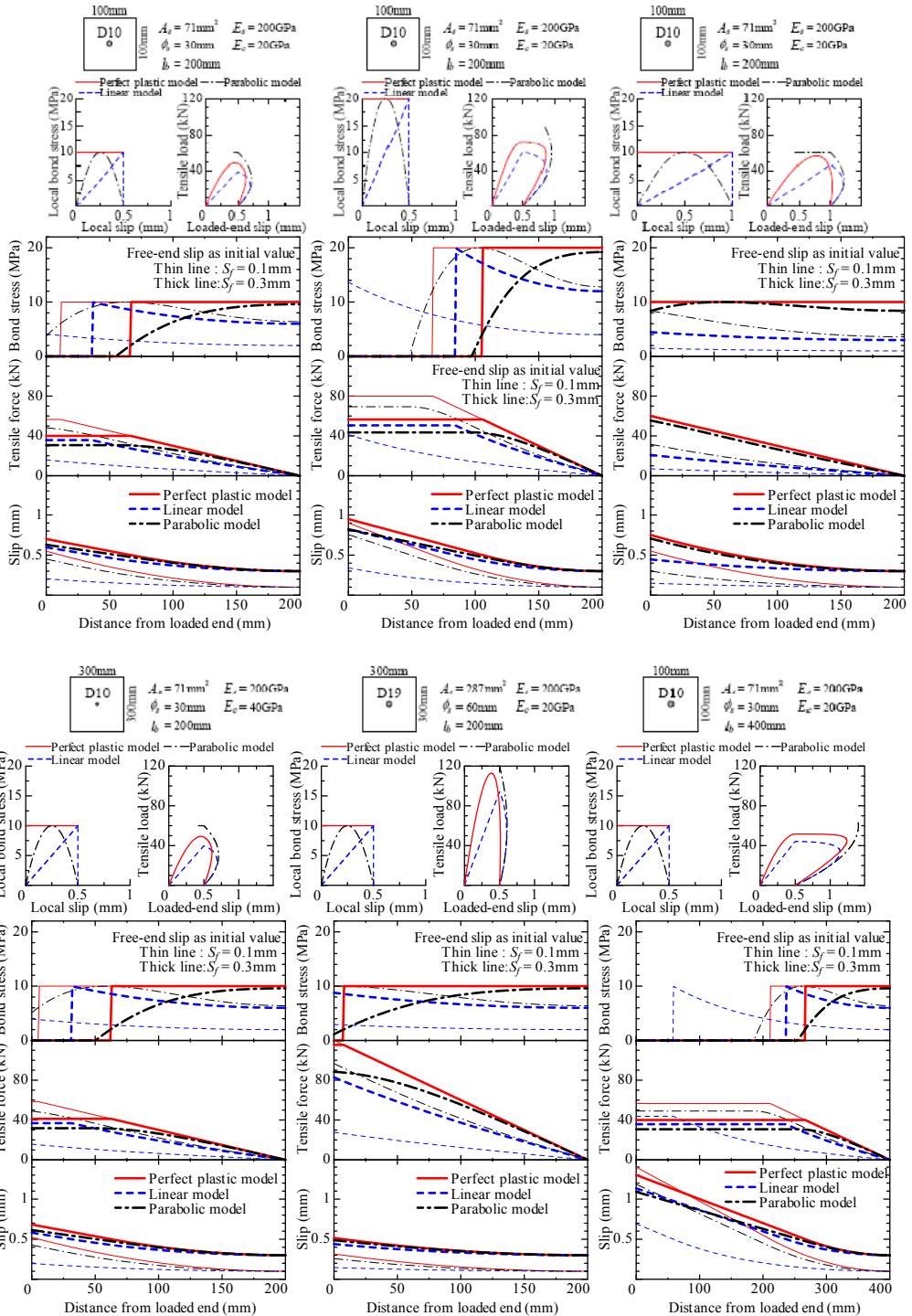


Figure 5. Bond stress-slip model, Loaded-end tensile load versus loaded-end slip curve, Bond behavior in pullout specimen.

### 3.3 Bond strength in pullout specimen

To investigate the influence of local bond characteristics and various other factors on maximum tensile load of pullout specimen, sensitivity analysis is performed by using each model. Investigated factors are bond stress-slip model, bond length, reinforcing bar diameter, elastic modulus of reinforcing bar and bond fracture energy. The relationship between maximum tensile load and bond length, reinforcing bar diameter, elastic modulus of reinforcing bar, and bond fracture energy for each model are shown in Figure 6. In addition, the specifications of analysis factors are shown in Figure 6. In case of the investigation of bond fracture energy, similarity shape for all bond stress-slip models are used. The maximum tensile load for the perfect rigid-plastic model and

the linear model is obtained by theoretical solution, whereas for the parabolic model one is obtained by numerical calculation. The theoretical equations of the maximum tensile load using the perfect rigid-plastic model and the linear model in pullout specimen are as shown blow.

(A) Perfect rigid-plastic model

$$P_{so,max} = \phi_s \cdot \tau_m \cdot l_b \leq \sqrt{\frac{2 \cdot E_s \cdot A_s \cdot \phi_s}{1 + np}} \cdot \tau_m S_u \quad (5)$$

(B) Linear model

$$P_{so,max} = \sqrt{\frac{2 \cdot E_s \cdot A_s \cdot \phi_s}{1 + np}} \cdot \frac{1}{2} \tau_m S_u \cdot \left( \frac{e^{2\alpha b} - 1}{e^{2\alpha b} + 1} \right) \quad (6)$$

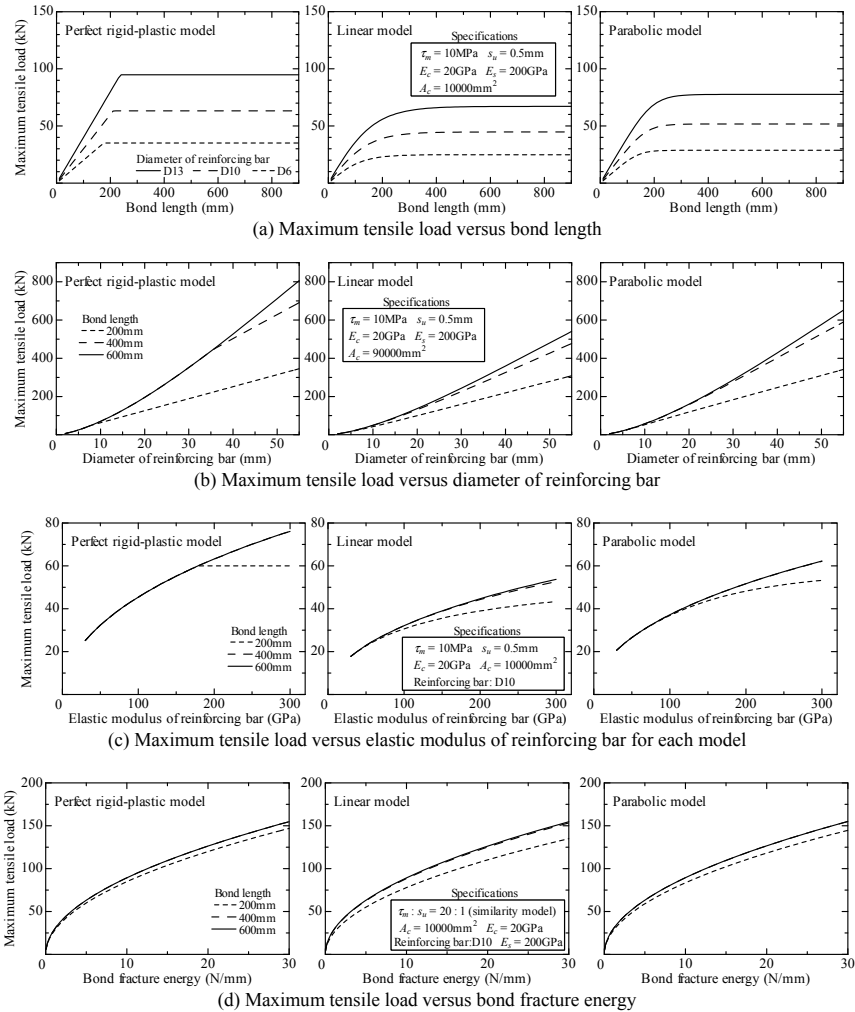


Figure 6. Maximum tensile load in pullout specimen.

where  $\alpha = \sqrt{\frac{k \cdot (1+np) \cdot \phi_s}{E_s \cdot A_s}} = \sqrt{\frac{(1+np) \cdot \phi_s \cdot \tau_m}{E_s \cdot A_s \cdot S_u}}$ ,  $\tau_m$  = local

bond strength,  $k$  = bond stiffness,  $S_u$  = ultimate slip, and  $l_b$  = bond length.

The maximum tensile load increases linearly up to about 200mm bond length, and remains constant as bond length becomes longer. In case of longer bond length, the perfect rigid-plastic model gives the highest maximum tensile load, followed by the parabolic model and, finally, the linear model, and also main features are similar to those for various reinforcing bar diameter. As the diameter of reinforcing bar sizes up, the maximum load increases linearly in case of shorter bond length and one increases nonlinearly in case of longer bond length. The maximum tensile load is proportional to square root of bond fracture energy and the elastic modulus of reinforcing bar.

When the bond length is sufficiently large and the concrete deformation is negligibly small, the maximum tensile load can be expressed by bond fracture energy, reinforcing bar perimeter, reinforcing bar area and elastic modulus of the reinforcing bar, as shown in Equation 7. (Asano et al. 2008)

$$P_{max} = \sqrt{\frac{2 \cdot E_s \cdot A_s \cdot \phi_s \cdot G_{fb}}{1+np}} \quad (7)$$

Where  $G_{fb}$  = bond fracture energy, which expressed as (A) Perfect rigid-plastic model:  $G_{fb} = \tau_m \cdot S_u$ , (B) Linear model:  $G_{fb} = (1/2) \cdot \tau_m \cdot S_u$ , (C) Parabolic model:  $G_{fb} = (2/3) \cdot \tau_m \cdot S_u$ .

In addition, the condition of bond length for maximum tensile load to achieve the value of Equation 7 can be expressed roughly as shown in Equation 8, which is derived from Equation 5. (Yasojima et al. 2003) Furthermore, the right-hand side in Equation 8 (i.e. the effective bond length) is defined as the region where comparatively effective bond stress distributes.

The effective bond length computed with the analysis specifications for reinforcing bar diameter D10 in Figure 6(a) is 211mm for the perfect rigid-plastic model, 298mm for the linear model, and 258mm for the parabolic model. It is confirmed that the maximum tensile load is constant in the bond length beyond those.

$$l_b \geq S_u \cdot \sqrt{\frac{2 \cdot E_s \cdot A_s}{(1+np) \cdot \phi_s \cdot G_{fb}}} \quad (8)$$

Where  $l_b$  = bond length,  $G_{fb}$  = bond fracture energy ( $= \tau_m \cdot S_u$ ),  $S_u$  = ultimate slip,  $E_s$  = elastic modulus of reinforcing bar,  $A_s$  = reinforcing bar area,  $\phi_s$  = perimeter of reinforcing bar,  $n$  = ratio of the elastic modulus ( $= E_s/E_c$ ),  $p$  = ratio of area ( $= A_s/A_c$ ),  $E_c$  = elastic modulus of concrete,  $A_c$  = concrete cross-sectional area.

## 4 SUMMARY AND CONCLUSIONS

Sensitivity analytical results in tensile specimen show that the influence of differences of local bond stress-slip model is relatively small for the linear model and the parabolic model, and the shape of slip distribution for all the models is similar.

Sensitivity analytical results in pullout specimen show that the influence of differences of local bond stress-slip model is relatively small in the distribution of tensile force and of slip, and the bond stress distribution differs among the models.

When the local bond strength and the bond stiffness vary, the length where the bond stress occurs significantly varies in all the models, and it is confirmed that the cross sectional area of specimen and the elastic modulus of concrete don't affect the respective distributions and the maximum tensile load.

The maximum tensile load in pullout specimen is mainly influenced by bond fracture energy, reinforcing bar perimeter, reinforcing bar area and elastic modulus of the reinforcing bar, which is proportional to square root of bond fracture energy and the elastic modulus of reinforcing bar, and becomes constant as bond length increases.

## ACKNOWLEDGEMENT

The authors fully acknowledge the members of Japan Concrete Institute Technical Committee on Bond in Concrete Structures for their dedicated activities.

## REFERENCES

- Asano, K., Yasojima, A., Kanakubo, T., 2008: Study on BondSplitting Behavior of Reinforced Concrete Members: Part 6 Theoretical solution by the parabolic model of bond constitutive law, Journal of Structural and Construction Engineering, Transactions of Architectural Institute of Japan, 73(626), 641-646
- Yasojima, A., Kanakubo, T., 2003: Study on BondSplitting Behavior of Reinforced Concrete Members: Part 3 Predicting equation for bond splitting strength without lateral reinforcement, Journal of Structural and Construction Engineering, Transactions of Architectural Institute of Japan, (567), 117-123